

Transmission Line Differential Protection with Fuzzy Signal Processing Support

Waldemar Rebizant¹, Krzysztof Solak¹

¹Wroclaw University of Technology, Wybrzeze Wyspianskiego 27, 50-370 Wroclaw, Poland
waldemar.rebizant@pwr.wroc.pl, krzysztof.solak@pwr.wroc.pl

Abstract

This paper presents a new differential protection scheme for transmission lines with application of fuzzy signal processing. Traditional differential relays may have problems with proper classification of external faults with CT saturation. Better protection stabilization for such cases is obtained with support of fuzzy signal processing. In proposed solution the input signals as well as the standard percentage characteristic are fuzzified. The performance of presented fuzzy protection scheme has been tested with the signals generated with use of EMTP-ATP program and compared to the traditional solution.

1. Introduction

Differential protection is a commonly accepted protection of single and parallel transmission lines, if only appropriate communication link connecting all line terminals is available [1, 2, 3]. The zone of action of differential relay embraces only protected object, which means that differential relay should trip for internal faults only and restrain for all external disturbances. In standard solutions the stabilized characteristic (Fig. 1) is applied and the trajectory of differential/bias currents is tracked with respect to the relay characteristic to determine whether or not to trip the transmission line [2].

The standard differential relay percentage curve is determined by four protection settings, [2]: $I_{d0}=0.3I_n$, $I_{s2}=2I_n$, $k_1=0.3$ and $k_2=1.5$ (specific values used for testing purpose). The tripping is initiated if:

$$|I_d| \geq I_{op} = k_1 \cdot |I_{bias}| + I_{d0} \quad \text{for } |I_{bias}| \leq I_{s2} \quad (1)$$

$$|I_d| \geq I_{op} = k_2 \cdot |I_{bias}| - (k_2 - k_1) \cdot I_{s2} + I_{d0} \quad \text{for } |I_{bias}| \geq I_{s2} \quad (2)$$

with

$$I_d = |\dot{i}_S + \dot{i}_R| \quad I_{bias} = \frac{|\dot{i}_S| + |\dot{i}_R|}{2} \quad (3)$$

where: \dot{i}_S and \dot{i}_R being currents measured at line terminals, I_{bias} – amplitude of bias current, I_d – amplitude of differential current, I_{op} – relay operating current, I_n – line nominal load current.

The majority of external faults are usually not a big problem for the differential relay. Generally, CT errors due to saturation during external faults are compensated for by conventional stabilized characteristic with adequate slope setting. However, when there is a mismatch in CTs' load or they have non-identical magnetizing characteristics, a possibility still exists that one of the CTs saturates and not the other, which may lead to unwanted protection reaction [4].

Several approaches may be found in the literature, that according to the authors, should improve performance of the line differential relays. The solution presented in [3] is based on zero-sequence component for detection of current transformer saturation. The idea described in [5] makes use of adaptive time-dependent restraint coefficients that define the shape of percentage differential curve. Since the two cited solutions do not guarantee proper operation of the relay for all conditions either, new protection ideas are still needed to assure improved protection performance. The newly proposed solution fulfills the above requirements, with simultaneously maintained sensitivity and operation speed for internal faults calling for prompt tripping.

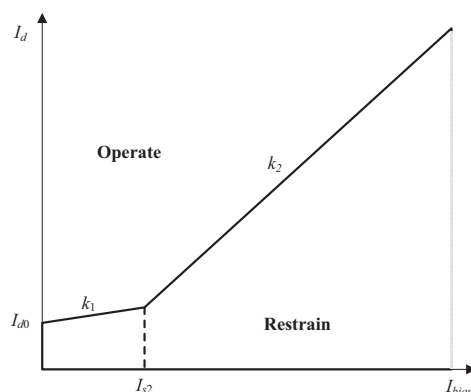


Fig. 1. Stabilized characteristic of the current differential relay

2. Fuzzy protection scheme developed

Classical (Boolean) logic based on the concept of truth/falsity cannot effectively cope with the many ambiguities that arise during operation of the power system. Therefore, fuzzy logic is increasingly being used in decision-making, whereas the criteria signals are described by membership functions. The use of fuzzy logic increases the confidence of the decision-making within an area of uncertainty, since the fuzzy logic can deal better (as compared to Boolean logic) with suspense and missing data. In addition, inferencing with multiple objectives in such systems is a natural way of processing information – it is therefore utterly possible to use numerous criteria in parallel.

Fig. 2 presents the structure of the new fuzzy protection. The main idea of action relies on fuzzification of differential current I_d that is further compared with fuzzy setting obtained on the basis of the stabilized characteristic (Fig. 1). Additionally, the criterion of phase difference is determined, value of which

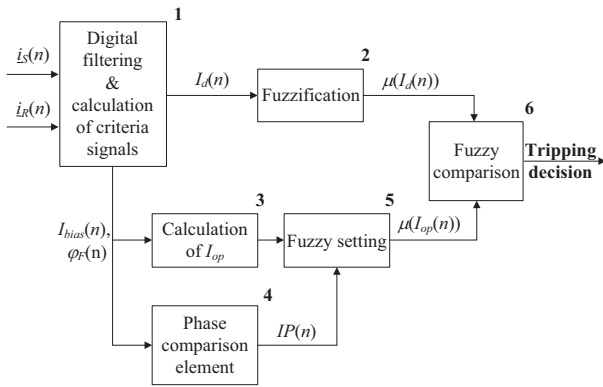


Fig. 2. Block scheme of the fuzzy adaptive differential protection of transmission line

affects the degree of fuzzification of fuzzy setting. Below the various blocks of scheme from Fig. 2 are described in detail.

Digital filtering and calculation of criteria signals (block 1) – here the main criteria signals (differential current I_d (3), bias current I_{bias} (3) and phase difference φ_F) are calculated with use of full cycle Fourier filters. The variable φ_F can be expressed by the formula:

- for asymmetrical faults it is calculated on the basis of negative sequence current since it gives excellent fault discrimination for such faults [6]:

$$\varphi_F = 180^\circ - \left| \arg \frac{i_{2S}}{i_{2R}} \right| \quad (4)$$

- unfortunately, the negative sequence current can not provide three-phase faults identification. Therefore, for symmetrical faults the phase difference is calculated on the basis of positive sequence current as follows:

$$\varphi_F = 180^\circ - \left| \arg \frac{i_{1S}}{i_{1R}} \right| \quad (5)$$

A three-phase fault is detected using overcurrent element tracking the level of bias currents in all phases.

Symmetrical components of the signals can be calculated according to the well known matrix formula:

$$\begin{bmatrix} \dot{i}_{0S(R)} \\ \dot{i}_{1S(R)} \\ \dot{i}_{2S(R)} \end{bmatrix} = \frac{1}{3} \begin{bmatrix} 1 & 1 & 1 \\ 1 & a & a^2 \\ 1 & a^2 & a \end{bmatrix} \begin{bmatrix} \dot{i}_{L1S(R)} \\ \dot{i}_{L2S(R)} \\ \dot{i}_{L3S(R)} \end{bmatrix} \quad (6)$$

where: $a = \exp(j2\pi/3)$, $\dot{i}_{0S(R)}$, $\dot{i}_{1S(R)}$, $\dot{i}_{2S(R)}$ – zero, positive, negative sequence currents at the S and R ends of the line, $\dot{i}_{L1S(R)}$, $\dot{i}_{L2S(R)}$, $\dot{i}_{L3S(R)}$ – phase currents at the S and R ends of the line.

Measuring of phase difference is initiated when the differential current is greater than or equal to I_{d0} in any phase.

Fuzzification (block 2) – magnitude of differential current (3) is fuzzified, which means that triangular membership functions is formed by using minimum I_{min} , average I_{av} and maximum I_{max} values of differential current (it was assumed that these values were calculated for a quarter of fundamental frequency cycle):

$$I_{min}(n) = \min_{k=0+(N/4)-1} \{I_d(n-k)\} \quad (7)$$

$$I_{av}(n) = \frac{1}{N/4} \sum_{k=0}^{(N/4)-1} I_d(n-k) \quad (8)$$

$$I_{max}(n) = \max_{k=0+(N/4)-1} \{I_d(n-k)\} \quad (9)$$

where: N – measuring window length (here $N=20$).

An example of how the fuzzification of differential current proceeds is shown in Fig. 3. Based on five samples of magnitude of differential current (Fig. 3a) the adequate values are calculated according to equations (7), (8) and (9). Next, the triangle membership function is formed as shown in Fig. 3b.

Calculation of I_{op} (block 3) – the value of operation current is calculated according to equations (1) and (2) – based on bias current I_{bias} .

Phase comparison element (block 4) – here the calculated phase difference, (4) or (5), is compared with the operation characteristic (see Fig. 4). The adequate threshold values of the characteristic have been set according to the statistical

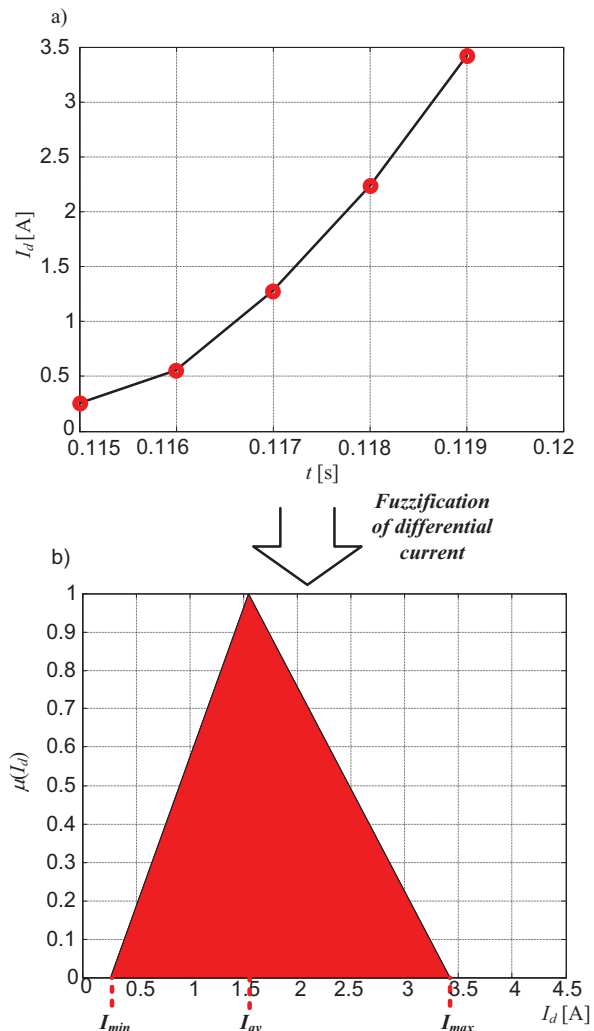


Fig. 3. Fuzzification of differential current: a) magnitude of differential current, b) fuzzy differential current

information gained through analysis of generated simulation signals. The output value IP from phase comparison element influences fuzzification of operation current. If the output value is close to 1.0 it indicates an external fault. Otherwise (internal fault cases) the output is close to 0.0.

Fuzzy setting (block 5) – based on the actual value of operation current and information from phase comparison block the fuzzy setting is formed as it is illustrated in Fig. 5. The parameters δ_1 and δ_2 determine the fuzzification of membership function of fuzzy setting and they can be calculated according to:

$$\delta_1 = IP \cdot I_{bias} + 0.1 \quad \delta_2 = 1.5 \cdot IP \cdot I_{bias} + 0.3 \quad (10)$$

The values of parameters in (10) are small ($\delta_1=0.1$ and $\delta_2=0.3$) for $IP=0$ (this value indicates internal fault) which means that membership function is slightly fuzzy. When $IP=1$ (this value indicates external fault) both parameters are high and the membership function of fuzzy setting is quite broad.

Fuzzy comparison (block 6) in this block both membership functions fuzzy differential current $\mu(I_d)$ and fuzzy setting $\mu(I_{op})$ are compared with each other (Fig. 6). The value of fuzzy comparison is determined by relation (11), where P - the area under the membership function of differential current $\mu(I_d)$

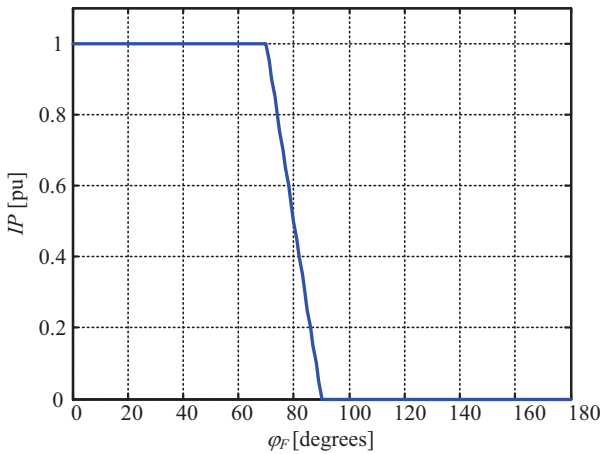


Fig. 4. Operation characteristic for phase difference

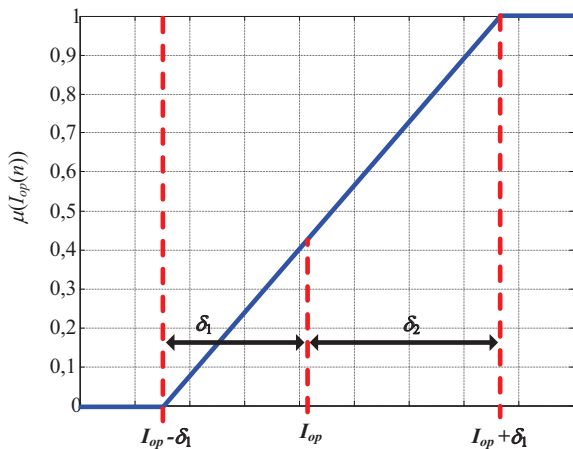


Fig. 5. Formation of fuzzy setting

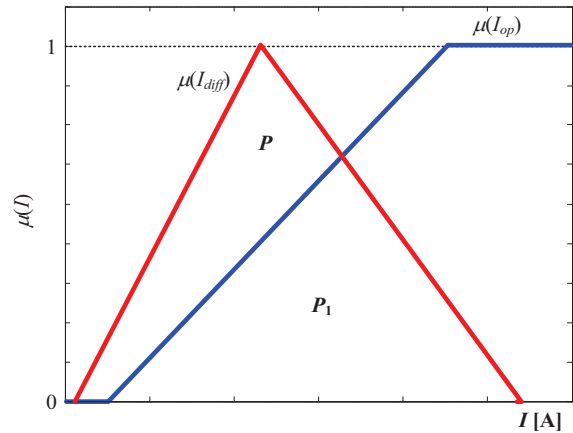


Fig. 6. Fuzzy comparison illustration

and P_d - surface area (hatched) lying under a fuzzy setting $\mu(I_{op})$, but within $\mu(I_d)$, [7].

$$P_d = \frac{\int \min[\mu(I_d), \mu(I_{op})] dI}{\int \mu(I_d) dI} = \frac{P}{P_1} \quad (11)$$

The final decision to trip a protected transmission line is taken when the value of index P_d is greater than threshold 0.7.

3. Testing of developed fuzzy protection scheme

The idea presented above has been subjected to extensive simulative testing in order to prove its efficiency. The basic system with HV transmission line under study is shown in Fig. 7. The overhead transmission line is modeled as transposed one with distributed parameters frequency dependent JMarti model [8, 9]. The line of 50km length can be divided into two sections, so that internal faults (F_L) at almost arbitrary location along the line can be simulated. External faults are those modeled at busbars (location $F_{BS(R)}$ in Fig. 7).

The line is supplied from both sides, where the sending equivalent system is assumed to be strong (of high short-circuit power), while the receiving one is weaker. The power flow can be controlled by variable angle of the receiving source.

The transient response of CTs and the correct models in ATP-EMTP simulation are very important for the evaluation of high-speed relaying systems [10]. The 5P30 20VA 1000/1A CTs were modeled using the TYPE-96 pseudo-nonlinear element. In this model there is a possibility to set the residual

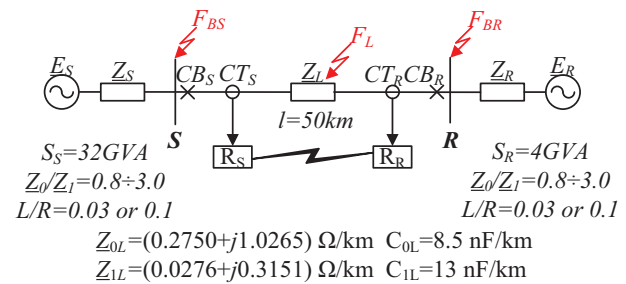


Fig. 7. Model of the power system with transmission

flux in the CT core, which is very important for studying CT saturation effects [3].

Thorough studies have been performed by varying the 400kV power system parameters, which resulted in over 20000 different simulation cases. The parameters being changed as systems strength, fault type, fault resistance, point on wave, residual flux, etc.

The figures below present testing results fuzzy scheme proposed and standard differential relay [2] for internal and external fault with CT saturation.

In Figs. 8-11 an example of three phase external fault at busbar F_{BR} with CTs saturation is presented. The CTs get saturated especially in phase L1 at sending end (Fig. 8) and the standard protection based on the stabilized characteristic with fixed settings maloperates, since the differential-restraining trajectory (phase L1) enters the tripping zone (Fig. 9) and the trip command is sent to the circuit breakers (Fig. 10a). On the contrary, proposed algorithm remained fully stable without issuing false tripping command – it effectively blocks this external fault (Fig. 10b).

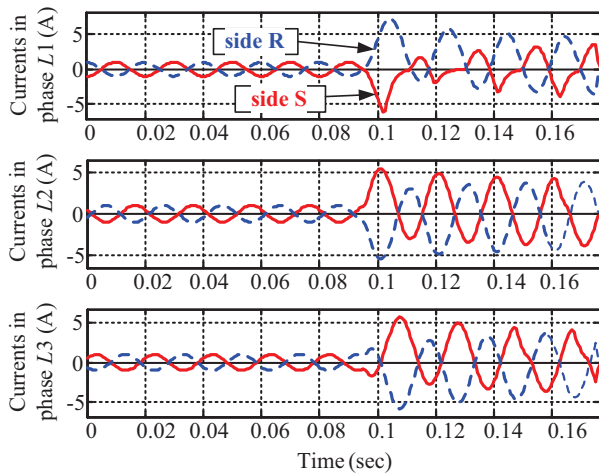


Fig. 8. Line terminal current wavelshapes in case of L1-L2-L3 external fault at busbar (F_{BR})

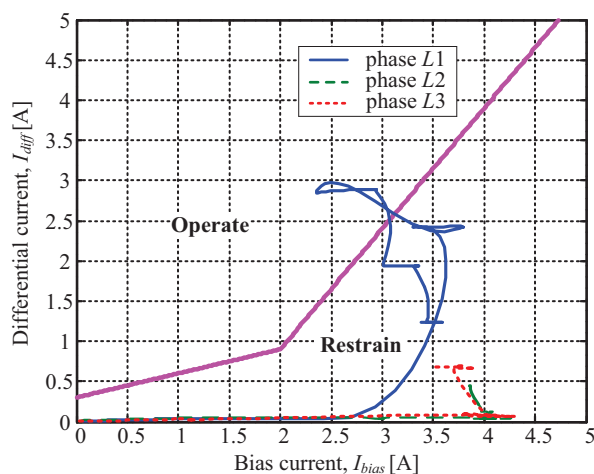


Fig. 9. Line protection stabilized characteristic and I_d-I_{bias} trajectory in case of L1-L2-L3 external fault at busbar (F_{BR})

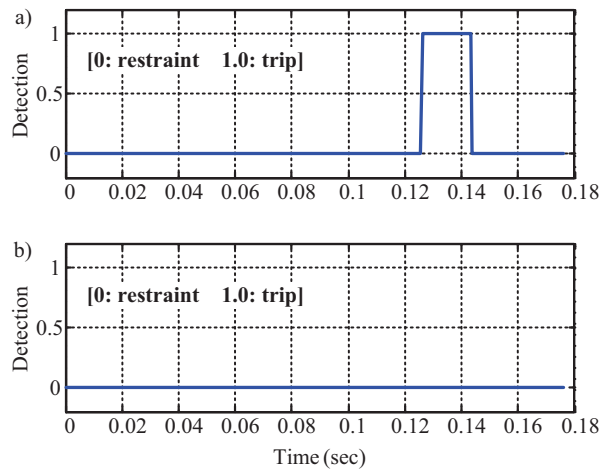


Fig. 10. Relay response for L1-L2-L3 external fault (F_{BR}): a) standard differential protection, b) fuzzy differential protection

The relaying schemes were tested for more than 3000 external fault cases obtained from EMTF simulation. The testing results proved that the proposed scheme is immune to external faults (zero percent of incorrect operation). Contrary, the standard protection failed for a few percent of external fault cases.

The developed adaptive protection scheme has also been tested for the cases of internal faults, for which unambiguous tripping command should be issued. A case of L1-L2-L3 internal fault (fault resistance 0Ω) at point F_L (fault location 7km from the sending end) is shown in Figs. 11-13. One can notice that when an internal fault occurs the CTs at the sending end deeply saturate (Fig. 11). The trajectory I_d-I_{bias} enters the tripping zone for all three phases and standard protection properly detects this case (Fig. 13a). The two algorithms (standard and proposed) detect this internal fault within less than 5ms after fault inception.

After analysis of testing results of both protection for over 21000 simulated internal fault cases one can say that average time detection of both protections are quite similar.

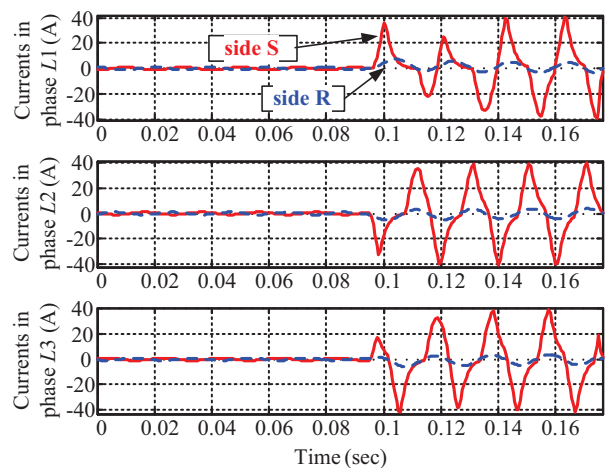


Fig. 11. Line terminal current wavelshapes in case of L1-L2-L3 internal fault at point F_L

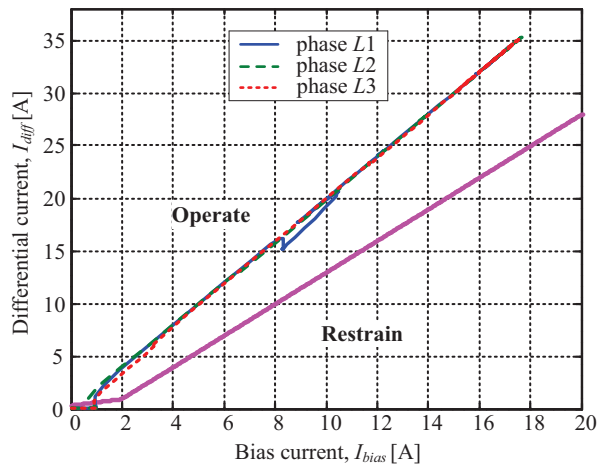


Fig. 12. Line protection stabilized characteristic and I_d-I_{bias} trajectory in case of $L1-L2-L3$ internal fault at point F_L

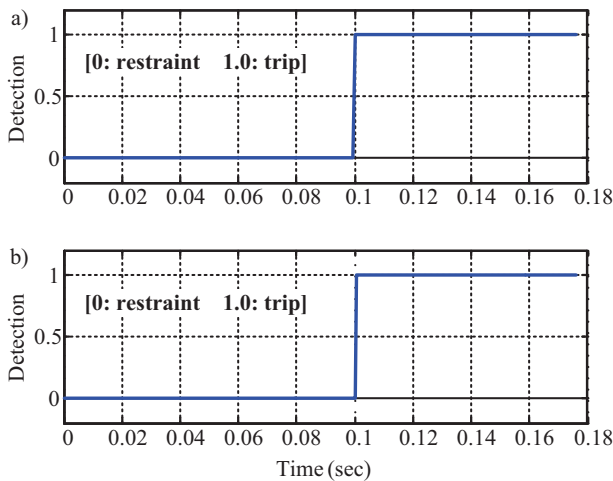


Fig. 13. Relay response for $L1-L2-L3$ internal fault (F_L):
 a) standard differential protection, b) fuzzy differential protection

4. Conclusions

The solution for improvement of the line differential protection under external fault cases is described in this paper. The results of fuzzy protection performance testing prove that the proposed algorithm remains fully immune to current transformer saturation during external faults. The proposed algorithm is also able to detect internal faults, even those with severe CT saturation within the same time like traditional solutions.

5. References

[1] S. Ward, T. Erwin, "Current Differential Line Protection Setting Considerations", *RFL Electronics Inc*, 2005.
 [2] AREVA, "P54x Application Guide", 2005.
 [3] N. Villamagna, P.A. Crossley, "A CT Saturation Detection Algorithm Using Symmetrical Components for Current Differential Protection", *IEEE Transactions on Power Delivery*, vol. 21, No. 1, pp. 38-45, January 2006.

[4] I. Voloh, B. Kasztenny, C.B. Campbell, "Testing line current differential relays using real-time digital simulators," in *Proc. 2001 IEEE/PES Transmission and Distribution Conference and Exposition*, pp. 516 – 521.
 [5] Gang W., Baoji Y., Jiali H., Li K.K.: "Implementation of Adaptive Dispersed Phase Current Differential Protection for Transmission Lines", *Proceedings of the 5th International Conference on Advances in Power System Control, Operation and Management*, APSCOM 2000, Hong Kong, October 2000, pp. 64 - 69.
 [6] Kasztenny B., Voloh I., Udrean E.A.: "Rebirth of the Phase Comparison Line Protection Principle", *59th Annual Conference for Protective Relay Engineers*, 4-6 April 2006, pp. 193 – 252.
 [7] Rebizant W., Wiszniewski A., Schiel L.: "Acceleration of Transformer Differential Protection with Instantaneous Criteria", *Proceedings of International Conference on Advanced Power System Automation and Protection*, Korea, 24-27 April 2007, CD-ROM, paper 505.
 [8] H.W. Dommel, "Electromagnetic Transients Program. Reference Manual (EMTP theory book)", Bonneville Power Administration, Portland 1986.
 [9] J.R. Marti, "Accurate modelling of frequency-dependent transmission lines in electromagnetic transients simulation", *IEEE Trans. Power App. Syst.*, vol. PAS-101, January 1982, pp. 147–157.
 [10] D.A. Tziouvaras, P. McLaren, G. Alexander et. al.: "Mathematical Models for Current, Voltage and Coupling Capacitor Voltage Transformers", *IEEE Transactions on Power Delivery*, Vol. 15, No. 1, January 2000, pp. 62 - 72.